Journal of Hydrology 420–421 (2012) 380–390

Contents lists available at SciVerse ScienceDirect

Journal of Hydrology

journal homepage: www.elsevier.com/locate/jhydrol

Simple modeling of the global variation in annual forest evapotranspiration

Hikaru Komatsu[a,b,*], Jaeil Cho[a], Kazuho Matsumoto[a,c], Kyoichi Otsuki[a]

[a] Kasuya Research Forest, Kyushu University, 394 Tsubakuro, Sasaguri, Kasuya, Fukuoka 811-2415, Japan
[b] School of Forestry and Resource Conservation, National Taiwan University, Taipei 106, Taiwan
[c] Faculty of Agriculture, University of the Ryukyus, Chihara 1, Okinawa 903-0213, Japan

ARTICLE INFO

Article history:
Received 10 June 2011
Received in revised form 5 December 2011
Accepted 16 December 2011
Available online 24 December 2011
This manuscript was handled by Andras Bardossy, Editor-in-Chief, with the assistance of Purna Chandra Nayak, Associate Editor

Keywords:
Forest evapotranspiration
Global scale
Hydrological cycle
Potential evaporation
Precipitation
Temperature

SUMMARY

Annual forest evapotranspiration (*ET*) is highly variable among various sites. Zhang's model (Zhang et al., 2001) has been widely used for predicting the spatial variation in *ET*. The forest component of the model employs limiting theory and assumes constant annual potential evaporation (E_0 = 1410 mm) by regressing data recorded at 56 forest sites. However, most of the data used in determining E_0 were recorded for limited regions (Australia, African countries, and the United States). We summarized 829 forest *ET* data items obtained for sites around the world from earlier publications. Using the dataset, we showed that Zhang's model overestimates forest *ET* in temperate and boreal regions with low annual mean temperature (*T*) owing to the E_0 value. We revised the E_0 term of Zhang's model so as to consider the dependency of E_0 on *T* using the dataset. The revised model did not overestimate forest *ET* in temperate and boreal regions. Consequently, we recommend revising the E_0 term of Zhang's model when predicting forest *ET* in these regions.

1. Introduction

Forests are one of the major biomes around the world (Hansen et al., 2003), and return a large portion of precipitation water to the atmosphere through evapotranspiration (Bosch and Hewlett, 1982; Zhang et al., 2001). Thus, forest evapotranspiration greatly affects the global and regional climate (Bala et al., 2007; Bonan, 2008) and river flow (Bosch and Hewlett, 1982; Brown et al., 2005), which further influence water resources, flooding, and sediment transport (Syvitski et al., 2005; Oki and Kanae, 2006; Bradshaw et al., 2007). In addition, forest evapotranspiration relates to carbon fixation (Leuning, 1990, 1995; Law et al., 2002) and biodiversity of the forest (Hawkins et al., 2003; Kreft and Jetz, 2007).

Forest evapotranspiration has been observed at numerous sites globally (Ruprecht et al., 1991; Kosugi and Katsuyama, 2007; Komatsu et al., 2008a; Matsumoto et al., 2008). Annual evapotranspiration (*ET)* has been found to be highly variable among various forest sites primarily owing to variations in meteorological conditions such as precipitation and potential evaporation (Zhang et al., 2001; Komatsu et al., 2008b). *ET* accounted for less than 20% of annual precipitation (*P*) at a Japanese site, where *P* was 2405 mm (Komatsu et al., 2008a). *ET* accounted for more than 90% at an Australian site, where *P* was 1179 mm (Ruprecht et al., 1991). Therefore, examining the spatial variation in forest *ET* is necessary to clarify the functional performance of forests in global and regional water cycles.

Many models (Budyko, 1974; Zhang et al., 2001; Gerten et al., 2004) have been proposed to predict the spatial variation in *ET*. These models are roughly classified into two groups according to complexity. The simple models generally employ limiting theory and the concept of potential evaporation (Schreiber, 1904; Budyko, 1974; Turner, 1991; Zhang et al., 2001) and/or regression of observed *ET* data (Lu et al., 2003; Komatsu et al., 2008b, 2010a; Sun et al., 2011). The complex models employ more process-based formulations including the Penman–Monteith equation or the bulk equation (Gerten et al., 2004; Mu et al., 2007; Jung et al., 2010; Zhang et al., 2010). The simple and complex models have different advantages. The simple models require data for only a few meteorological components at a coarse time resolution (e.g., annual precipitation (*P*), annual mean temperature (*T*), and annual net radiation) and require no (or little) information about forest properties such as forest type (i.e., broadleaf/coniferous and evergreen/deciduous), age, and leaf area index. Thus, these models have practical use (Sun et al., 2005, 2006; Brown et al., 2007) especially when available data are limited. The complex models formulate

* Corresponding author at: Kasuya Research Forest, Kyushu University, 394 Tsubakuro, Sasaguri, Kasuya, Fukuoka 811-2415, Japan. Tel.: +81 92 948 3109; fax: +81 92 948 3119.

E-mail address: kmthkr@gmail.com (H. Komatsu).

0022-1694/$ - see front matter © 2011 Elsevier B.V. All rights reserved.
doi:10.1016/j.jhydrol.2011.12.030

forest evapotranspiration as process-based functions of various meteorological components including radiation and humidity at high time resolution (e.g., daily time resolution) and the forest properties. Thus, these models are useful for predicting changes in evapotranspiration and water cycles with changing climate and vegetation (Gerten et al., 2004; Jung et al., 2010).

Among the simple models, Zhang's model (Zhang et al., 2001) has been widely used (Herron et al., 2002; Nordblom et al., 2006; Brown et al., 2007; Wang et al., 2008). Zhang's model expresses *ET* as a weighted average of forest and herbaceous components. The former component formulates forest *ET*, on the basis of data recorded at 56 sites in various regions (Zhang et al., 1999, 2001), as functions of *P* and annual potential evaporation (E_0). Similar to classic studies (Schreiber, 1904; Budyko, 1974), this model employs limiting theory and assumes that *ET* is limited by *P* where *P* is low and by E_0 where *P* is high. Although most classic studies (Schreiber, 1904; Budyko, 1974) formulate E_0 as functions of incident radiation and temperature, the forest component of Zhang's model assumes E_0 is a constant, which was determined as 1410 mm by regressing the data recorded at 56 forest sites. According to the constant-E_0 assumption, Zhang's model calculates forest *ET* with only the input of *P* data. This is a distinct advantage of this model for practical use, because radiation data are often unavailable for specific regions and in historical datasets (Hunt et al., 1998; Thornton and Running, 1999; Shinohara et al., 2007) and because radiation predicted from temperature and precipitation data could contain relatively large errors (Thornton and Running, 1999; Meza and Varas, 2000; Shinohara et al., 2007). Despite the simplicity of the model, it demonstrated high predictability for data recorded at the 56 forest sites. The simplicity and predictability led to the wide use of Zhang's model.

However, most of the data used by Zhang et al. (1999, 2001) for E_0 determination were recorded in limited regions (Australia, African countries, and the United States). Only a few data were for Asia, South America, Europe, and boreal regions, despite their large forested areas. Thus, the constant-E_0 assumption might not be useful for explaining the global variation in forest *ET*. Indeed, Komatsu et al. (2008b) noted that the model systematically overestimates forest *ET* in Japan, because Zhang's E_0 value is higher than that for Japan. Similar problems are expected for regions at high latitude, because E_0 for these regions would be no more than that for Japan (Budyko, 1974; Choudhury, 1997; Ward and Robinson, 2000). Their finding implies that applying the constant-E_0 assumption at a global scale is problematic.

This work extends Zhang's model to explain the global variation in forest *ET*. Using a comprehensive collection of *ET* observation data recorded around the globe, we show that predictability of Zhang's model is improved when considering the dependency of E_0 on *T*.

2. Materials and methods

2.1. Methods of analysis

Zhang's model formulates forest *ET* as (Fig. 1)

$$ET = P(1 + wE_0/P)/(1 + wE_0/P + P/E_0), \quad (1)$$

where *w* is a coefficient representing plant water availability. *w* and E_0 were determined as 2.0 and 1410 mm, respectively, by regressing the data recorded at 56 forest sites. Changes in *ET* with *P* are small where *P* is high (Fig. 1). This indicates small variations in *ET* among sites for regions with high *P*. *P* was greater than 2000 mm at nine sites among the data collected by Zhang et al. (2001). The mean and standard deviation of *ET* for the nine sites were 1353 and 107 mm, respectively. The mean value was approximately identical to the E_0 value determined by Zhang et al. (2001). The standard deviation accounted for only 8% of the mean value, suggesting the validity of the constant-E_0 assumption within the limit of the data they collected.

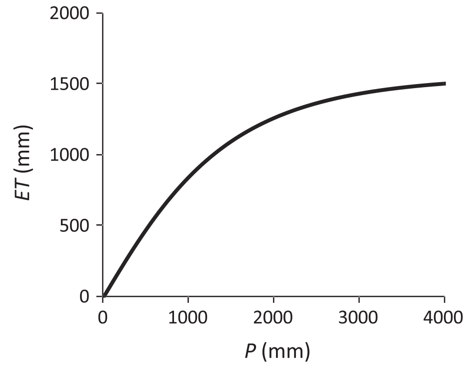

Fig. 1. Relationships of annual forest evapotranspiration (*ET*) with annual precipitation (*P*) predicted using Zhang's model.

We first collected forest *ET* data globally and showed that Zhang's model systematically overestimated forest *ET* especially for regions at high latitudes, because the E_0 value determined by Zhang et al. (1999, 2001) was too large for the regions. We then revised the E_0 term of Zhang's model to reduce the overestimation at high latitudes. For this, we classified *ET* data into different *T* classes and determined E_0 to minimize the root-mean-square error (RMSE) for *ET* estimates for each class. We further developed a map indicating the regions where Zhang's model overestimated forest *ET* and the use of the revised model is recommended. For this, we calculated global forest *ET* variations using the revised model and Zhang's model, respectively, and developed a map showing the difference between these two *ET* estimates. Additionally, we showed that the revised model was useful for predicting the difference in the sensitivity of forest *ET* to temporal variations in *P* among sites. The sensitivity for each site was evaluated using the slope of the linear regression line between *P* and *ET* during the measurement period for the site. A greater slope indicated that *ET* was sensitive to *P*. We compared the slope value derived from observations with that predicted using the revised model.

2.2. Evapotranspiration data

We collected forest *ET* data from earlier papers using three criteria. Firstly, *ET* must be determined from one or a combination of measurements of the catchment water balance (Pearce et al., 1982; Iroumé et al., 2006), soil water balance (Calder et al., 2003; Muller, 2009), micrometeorology (Wilson and Baldocchi, 2000; Oishi et al., 2010), porometry (Bigelow, 2001), sap flux (van Wijk et al., 2001; McJannet et al., 2007), and throughfall (Van der Salm et al., 2006; Huber et al., 2008). If *ET* data obtained using different methods were available for a specific site (Wilson et al., 2001; Shimizu et al., 2003), we treated these data independently. This treatment did not alter our results and conclusions, because only 10 sites satisfied this condition (i.e., *ET* data obtained using different methods were available for a specific site). Among the data derived from catchment water balance measurements, some data were derived from catchments that were not fully covered with forest. We accepted data only for catchments for which no less than 70% of the area was covered with forest. This definition of a forest catchment would generally agree with that used by Zhang et al. (1999, 2001), although they did not clearly state the definition. They also used data for catchments partially covered with forest (Sharda et al., 1998) for developing the forest component of their model. For some catchments, forest treatment such as clearcutting, thinning, and species conversion (e.g., conversion from broadleaf forests to coniferous plantation forests) was performed during the measurement period (Rowe and Pearce, 1994; Cornish and Vertessy, 2001; Komatsu et al., 2008a). In clearcutting cases, we used only data before clearcutting. In cases of thinning and species conversion, we excluded data during the treatment and used data before and after treatment independently.

Secondly, the period of evapotranspiration measurements must not be less than 1 year. In some cases (Amthor et al., 2001; Kumagai et al., 2004), although the original data period was less than 1 year, the data gaps were filled employing regression or process-based models, and therefore *ET* data were available. We also used these *ET* data for analysis. If *ET* data for no less than 2 years were available for a specific site (Gielen et al., 2010; Komatsu et al., 2010b), we used the mean *ET* value for the measurement years.

Thirdly, large errors in *ET* measurements were not pointed out in the original paper reporting *ET* data for a specific site. Some *ET* data derived using the catchment water balance (Maita et al., 2005) or sap-flux method (Wilson et al., 2001) were excluded on the basis of this criterion. Maita et al. (2005) pointed out that *ET* in their site derived using the catchment water balance method would be greatly overestimated owing to considerable percolation flux. Wilson et al. (2001) pointed out that *ET* in their site derived using the sap-flux method would be greatly underestimated owing to systematic errors in estimating sap flux for broadleaf tree species.

Consequently, we obtained 829 forest *ET* data from earlier publications (Table 1; Supplementary data). We got a good spread of sites with exception of Siberia (Fig. 2). The major portion of the data (631 data) was derived from catchment water balance measurements. However, a considerable portion was derived from micrometeorological or soil water balance measurements (81 and 63 data, respectively).

For additional analysis examining the sensitivity of forest *ET* to temporal variations in *P*, we selected data for which the measurement period was no less than 5 years and *P* variations among the years were considerable (i.e., the standard deviation of *P* is greater than 10% of the mean *P*). Consequently, we obtained 83 observation data among the 829 data (Table 2). The major portion of the data (75 data) was derived from catchment water balance measurements. A minor portion was derived from micrometeorological or soil water balance measurements (three and five data, respectively).

2.3. Global data of precipitation and temperature

To map the global forest *ET* variation using our revised model and Zhang's model, we prepared global data of *P* and *T* from the NCC database. This database includes a global climate dataset with temporal resolution of 6 h and spatial resolution of $1^\circ \times 1^\circ$ after elevation correction using NCEP/NCAR reanalysis data (Ngo-Duc et al., 2005). We converted the 6-hourly NCC data to annual values so that they could be used with our revised model and Zhang's model. The model calculations in this study spanning the 1990s are for only forest regions of the GLC2000 global land-cover map, which was obtained by global remote sensing and field observations in 2000 (Bartholomé and Belward, 2005). The forest *ET* value for each year during 1990–1999 was averaged to obtain the mean *ET* for the 1990s. Note that the 1990s matched the period for which many of the observations were available.

3. Results

3.1. Evaluation of Zhang's model

Fig. 3 shows the relationship between forest *ET* and *P* for regions with different latitude and longitude. Both *ET* and *P* were high at low latitude and low at high latitude. This qualitatively validates Zhang's model in that *ET* is higher for higher *P* in the model. However, the model is not valid quantitatively. Although data for low latitudes can be plotted along the line representing Zhang's model (Fig. 3; solid line), data for high latitudes tended to be below the line, falling to around 50% of the prediction. This clear latitude-dependent pattern might be due to the spatial variation in *T* and other meteorological components such as radiation. Note that most of the data summarized by Zhang et al. (1999, 2001) were derived for Australia, African countries, and the United States. Data for these areas lay near the line representing Zhang's model (Table 1, Fig. 3).

Fig. 4 shows the relationships between *ET* and *P* for different *T*. *ET* predicted using Zhang's model was comparable with observed *ET* for *T* no less than 20 °C (Fig. 4a). However, *ET* predicted using the model was higher than observed *ET* for *T* lower than 20 °C (Figs. 4b and 4c). These results suggest that modeling E_0 as a function of *T* could improve the predictability.

3.2. Revision of Zhang's model

We classified all data into nine classes according to *T* (the *T* range for each class was 5 °C). The nine classes were set as to cover the whole range of *T*. We determined E_0 values that minimized the RMSE for *ET* estimates for each class (Fig. 5). The E_0 value for *T* higher than 20 °C (E_0 = 1301–1507 mm) was comparable with Zhang's E_0 (= 1410 mm). However, the E_0 value for *T* no more than 20 °C (E_0 = 149–1077 mm) was lower than Zhang's E_0, indicating systematic overestimates of *ET* when using Zhang's model under these conditions. We determined a regression equation for the relationship between *T* and E_0 (Fig. 5; solid line) and obtained the equation

Table 1
Annual precipitation (*P*) and forest evapotranspiration (*ET*) for each longitudinal and latitudinal region.[a]

	180°W–30°W (North and South America)			30°W–60°E (Africa and Europe)			60°E–180°E (Asia and Oceania)		
	P (mm)	*ET* (mm)	Sample size	*P* (mm)	*ET* (mm)	Sample size	*P* (mm)	*ET* (mm)	Sample size
60°N–	374[b] (80[c])	246 (74)	14	640 (101)	305 (102)	40	412 (128)	167 (38)	5
40°N–60°N	1239 (633)	526 (170)	127	908 (394)	504 (160)	130	973 (517)	428 (135)	24
20°N–40°N	1290 (459)	755 (203)	136	495 (149)	478 (156)	4	1689 (760)	703 (224)	94
20°S–20°N	2780 (889)	1355 (371)	55	1768 (863)	1164 (281)	34	2577 (1057)	1255 (329)	57
40°S–20°S	1660 (758)	886 (322)	13	1609 (405)	927 (257)	10	1269 (359)	921 (221)	62
60°S–40°S							1892 (765)	829 (193)	24

[a] Original data are presented in Supplementary data.
[b] Mean values for the sites included within the longitudinal and latitudinal region.
[c] Standard deviation.

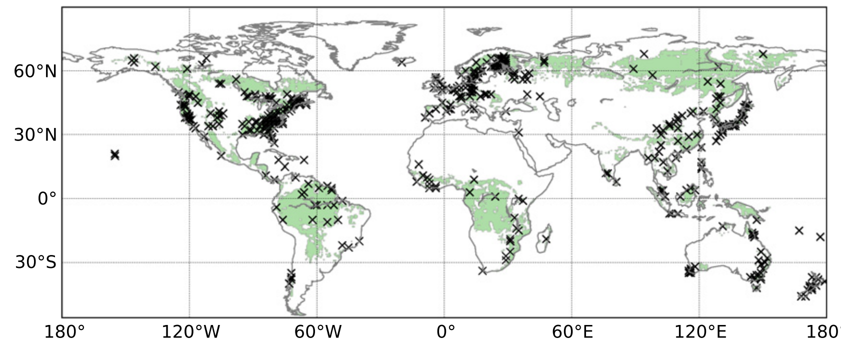

Fig. 2. Location of observation sites for the 829 forest evapotranspiration data (cross). The green areas indicate forested regions according to GLC2000 global land cover data for the year 2000 (Bartholomé and Belward, 2005).

Table 2
Sample size of data for determining the sensitivity of annual forest evapotranspiration (ET) to annual precipitation (P)[a].

	180°W–30°W (North and South America)	30°W–60°E (Africa and Europe)	60°E–180°E (Asia and Oceania)
60°N–	0	1	1
40°N–60°N	7	11	3
20°N–40°N	4	1	14
20°S–20°N	2	1	2
40°S–20°S	3	1	27
60°S–40°S			5

[a] Original data are presented in Supplementary data.

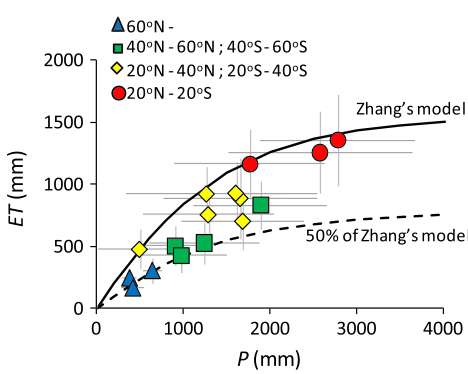

Fig. 3. Relationships of the mean annual evapotranspiration (ET) for forests with the mean annual precipitation (P) for different longitude and latitude regions. Bars indicate standard deviations. The solid line indicates forest ET being identical to that predicted using Zhang's model. The dotted line indicates forest ET being identical to the predicted ET multiplied by 0.5.

$$E_0 = 0.488T^2 + 27.5T + 412(R^2 > 0.99), \quad (2)$$

where E_0 and T have units of millimeters and degrees Celsius. The fact that E_0 varied with T agrees with previous theoretical and experimental studies that regarded temperature as a critical factor determining E_0 (Thornthwaite, 1948; Hamon, 1961; Komatsu et al., 2008b, 2010a). On the basis of the revision, the ET plateau of the model for high P changes according to the T value (Fig. 6). Note that we assumed w as 2.0, which was determined by Zhang et al. (2001). Validity of this assumption would be discussed in Section 4.3.

Because of this revision of E_0, the revised model did not systematically overestimate forest ET according to the 829 ET data points (Fig. 7a), which contrasts with the case for Zhang's model (Fig. 7b). The slope of the regression line for all data was 1.04 for the revised model and 0.830 for Zhang's model. Similarly, the revised model had higher R^2 and lower RMSE values (0.731 and 192 mm, respectively) than Zhang's model (0.473 and 353 mm, respectively) according to the 829 ET data. This difference in predictability was primarily due to the data for relatively low temperature. According to the data for $T < 20$ °C, the slope, R^2, and RMSE values were 1.06, 0.573, and 180 mm for the revised model. They were 0.578, 0.374, and 369 mm for Zhang's model. We here used the same data for the determination of E_0 and evaluation of model predictability (Figs. 5 and 7). Even when using half of the ET data to determine E_0 and the residual to evaluate model predictability, the higher predictability of the revised model was still observed (data not shown). Thus, this revision of Zhang's model is important for understanding the global variation in forest ET.

3.3. Regions where the revised model should be used

Fig. 8a and b shows global variations in forest ET predicted using the revised model and Zhang's model, respectively. The global pattern of forest ET predicted using the revised model was similar qualitatively to that predicted using Zhang's model. Higher ET values were observed at lower latitude in both cases. However, the patterns differed quantitatively. Fig. 8c shows the relative difference in ET predicted using the two models; i.e., the difference between ET values estimated using the revised model and Zhang's model divided by the ET value estimated using the revised model. The relative difference was larger at higher latitude, suggesting that the dependency of E_0 on T should be considered in these regions.

3.4. Sensitivity of ET to temporal variations in P

The sensitivity of forest ET to temporal variations in P was found to differ among sites. For the L'Avic site in Spain (Piñol et al., 1991), temporal variations in ET corresponded to those in P; i.e., ET was sensitive to P (Fig. 9a). For the Sarukawa II site in Japan (Takeshita et al., 1996), temporal variations in ET did not clearly correspond to those in P; i.e., ET was insensitive to P (Fig. 9b). The slope of the linear regression line between P and ET was greater ($p < 0.01$) for L'Avic than for Sarukawa II according to analysis of covariance (Fig. 9c). This difference was also predicted by the model. The mean P during the measurement years was 548 mm for L'Avic and 2766 mm for Sarukawa II. According to the model, the slope of the tangent line for P = 548 mm (Fig. 9d; dotted line) was greater than that for P = 2766 mm (Fig. 9d; broken line). Note that as T was nearly the same for these two sites, E_0 for these sites predicted using the model was nearly the same. Consequently, we used the same line representing the relationship between P and ET predicted using the model for these sites (Fig. 9d).

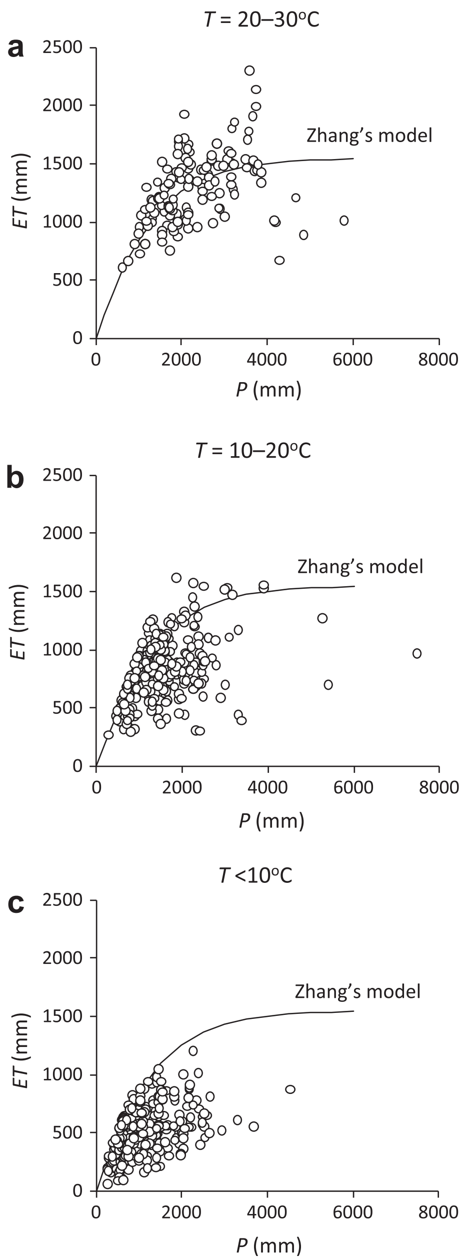

Fig. 4. Comparison of Zhang's model prediction and observation data. (a–c) Relationships between annual precipitation (*P*) and forest evapotranspiration (*ET*) for different mean annual temperature (*T*) classes.

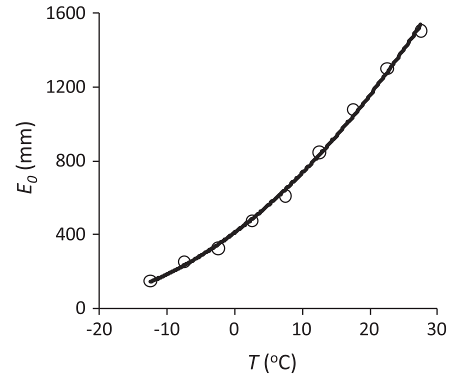

Fig. 5. Relationship between annual mean temperature (*T*) and annual potential evaporation (E_0), where E_0 was determined for each temperature class using the least-squares method. The solid line indicates the regression line determined using the least-squares method.

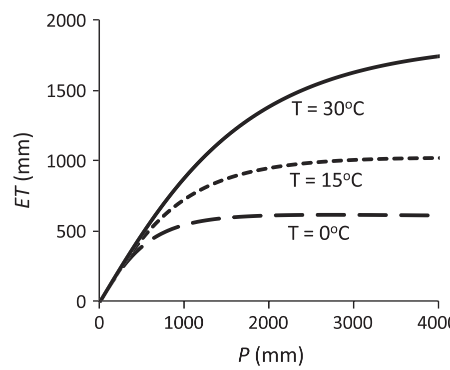

Fig. 6. Relationship between annual precipitation (*P*) and annual forest evapotranspiration (*ET*) for different annual mean temperatures (*T*) obtained using the revised model.

Numerically differentiating the equation for the model (Fig. 6) by *P*, we obtained the relationship indicated by the solid line in Fig. 10. The sensitivity of forest *ET* to *P* was found to relate to *ET*/*P* values regardless of *T*. Observation data for the 83 forest sites (Table 2) were plotted near the line representing the model results. These results indicate that the model was useful for explaining the difference in *ET* sensitivity to temporal *P* variations among sites, as well as predicting the spatial variation in *ET*.

4. Discussion

4.1. Effect of the measurement method

Most of the data we used in the analysis were derived using the catchment water balance method. This method introduces specific errors in *ET* estimates. The method calculates *ET* as the difference between *P* and annual runoff (Malmer, 1992; Kosugi and Katsuyama, 2007; Komatsu et al., 2007, 2008b). Thus, it assumes no percolation flux and can therefore overestimate *ET*. Furthermore, the method assumes no change in soil water storage and can therefore introduce large errors when applied to *P* and annual runoff at a short time-scale (e.g., 1 year). This error could be critical for the analysis of the sensitivity of *ET* to temporal *P* variations, because the analysis examines interannual variations in *ET* (Fig. 10). In addition, the spatial scale of *ET* data derived using the catchment water balance method varies largely among catchments (ranging between 10^{-2} and 10^{3} km). This contrasts with *ET* data obtained using other methods (e.g., the soil water balance and micrometeorological methods); the spatial scale of *ET* data obtained using other methods is relatively consistent (typically between 10^{-3} and 10^{-2} km). Thus, it is necessary to examine whether our results are dependent of the measurement method.

Figs. 11a and b are the same as Figs. 7a and 10, respectively, but plotted according to measurement method. In the case of Fig. 11a, the regression lines for data derived using the catchment water balance method and for data derived using the other methods are written as $y = 1.06x - 48.8$ ($R^2 = 0.756$) and $y = 1.02\ x - 23.4$ ($R^2 = 0.712$), respectively. The difference in the regression slope is not significant ($p > 0.05$) according to analysis of covariance. Note that the regression line for data derived using the catchment water balance with the measurement period $\geqslant$5 years is nearly the same as that for all data derived using the catchment water balance method (data not shown). In the case of Fig. 11b, the regression

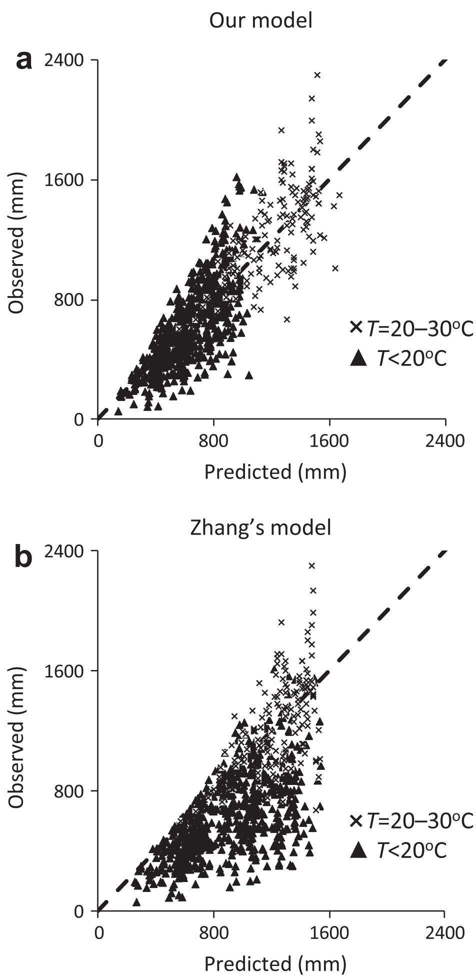

Fig. 7. Comparison (a) between annual forest evapotranspiration (*ET*) predicted using our revised model and observed *ET* and (b) between *ET* predicted using Zhang's model and observed *ET*. Data were classified according to annual mean temperature (*T*). The dotted line indicates the 1:1 relationship. The regression line for all data, determined using the least-squares method, was $y = 1.04\ x - 36.7$ ($R^2 = 0.731$) for our model and $y = 0.830x - 59.4$ ($R^2 = 0.473$) for Zhang's model. The regression line for data with $T < 20$ °C was $y = 1.06x - 52.4$ ($R^2 = 0.573$) for our model and $y = 0.578x + 109$ ($R^2 = 0.374$) for Zhang's model. The regression line for data with $T \geqslant 20$ °C was $y = 0.890x + 153$ ($R^2 = 0.400$) for our model and $y = 0.875x + 172$ ($R^2 = 0.312$) for Zhang's model.

lines for data derived using the catchment water balance method and data derived using the other methods are written as $y = 1.16x - 0.329$ ($R^2 = 0.699$) and $y = 1.13x - 0.438$ ($R^2 = 0.555$), respectively. The difference in the regression slope is not significant ($p > 0.05$) according to analysis of covariance. Thus, there is no evidence for the dependency of the results on the measurement method according to our data set. However, there are only seven data derived using the other methods in Fig. 11b. This suggests necessity of further examinations on the relationship between *ET*/*P* and the sensitivity of *ET* to *P* using a more comprehensive data set.

4.2. Scattering for similar T

Although the revised model demonstrated high predictability, there was still considerable scattering (Fig. 7a). This scattering is not classified by the forest type; i.e., broadleaf/coniferous (Fig. 12a) and evergreen/deciduous (Fig. 12b). In the case of Fig. 12a, the regression lines for data for broadleaf and coniferous forests are written as $y = 0.906\ x + 32.4$ ($R^2 = 0.620$) and $y = 0.962x + 82.1$ ($R^2 = 0.614$), respectively. In the case of Fig. 12b, the regression lines for data for evergreen and deciduous forests are written as $y = 1.03x - 1.30$ ($R^2 = 0.730$) and $y = 0.873x + 46.9$ ($R^2 = 0.562$), respectively. The differences in the regression slope are not significant ($p > 0.05$) according to analysis covariance.

We expect that there are two explanations for the above finding. First, the distribution of each forest type relates to meteorological conditions such as *P* and *T* (Thornthwaite, 1948; Melillo et al., 1993; Sitch et al., 2003). For example, broadleaf evergreen forests tend to be distributed in regions with high *T*, while broadleaf deciduous forests tend to be distributed in regions with low *T* (Melillo et al., 1993; Landsberg and Gower, 1997). We determined E_0 of the revised model for each *T* class using observation data (Fig. 5). Thus, if there was a difference in *ET* between broadleaf evergreen and deciduous forests, it would be implicitly included in E_0 of the model, and it could therefore be undetectable in analysis, such as in Fig. 12. Note that E_0 in the revised model (and also in Zhang's model) is not necessarily identical to the real value of potential evaporation (e.g., equilibrium evaporation). The revised model, as well as Zhang's model, assume that *ET* is controlled by E_0 and *P*. In reality, *ET* is also controlled physiologically. For example, stomatal closure and leaf fall due to temperature decline result in *ET* being less than equilibrium evaporation (Blanken et al., 1997; Wilson and Baldocchi, 2000; Arain et al., 2003). As E_0 in the model (and also that in Zhang's model) was determined by regressing observation data for *ET*, it corresponds to *ET* without water limitation but with other physiological control, such as stomatal closure and leaf fall due to temperature decline.

Second, there are various factors affecting *ET* besides the forest type; e.g., seasonality of precipitation and temperature and soil water capacity (Milly, 1994; Dooge et al., 1999). If this is the case, further classification of the scattered data according to the forest type might be possible for specific regions with similar seasonality of precipitation and temperature. For example, Komatsu et al. (2011) showed that the difference in *ET* between broadleaf deciduous and coniferous evergreen forests is apparent only for specific conditions of precipitation seasonality (i.e., high winter precipitation) on the basis of catchment water balance data obtained in the United States, New Zealand, and Japan. This suggests further classification according to forest type might be possible under specific conditions. We cannot examine such a possibility at this stage because we do not have enough data for the seasonality of precipitation and temperature and soil water capacity at the observation sites.

We also observed large underestimation of *ET* for several data with $T = 20–30$ °C (Fig. 7a). For example, there are two data with observed *ET* greater than 2000 mm (Schellekens, 2000; Loescher et al., 2005). These data were obtained for tropical rainforests in Puerto Rico and Costa Rica. *ET* predicted using the revised model was 1387 and 1564 mm, respectively, indicating extremely large underestimation by the model. The high *ET* values for these forests were primarily due to exceptionally high interception evaporation (Schellekens, 2000; Schellekens et al., 2000) and potential evaporation (Loescher et al., 2005), respectively. This suggests a limitation of predictability using a model that does not consider transpiration and interception evaporation separately and does not require inputs other than *P* and *T*.

4.3. Impact of w parameterization

When revising Zhang's equation, we determined E_0 but not the other parameter (w) using the 829 forest data we collected in this study. We assumed w as 2.0 following Zhang et al. (2001). In fact, E_0 and w in Zhang's model were simultaneously determined to minimize the error in *ET* estimates according to the 56 forest data collected by Zhang et al. (2001). Thus, it is possible to determine E_0

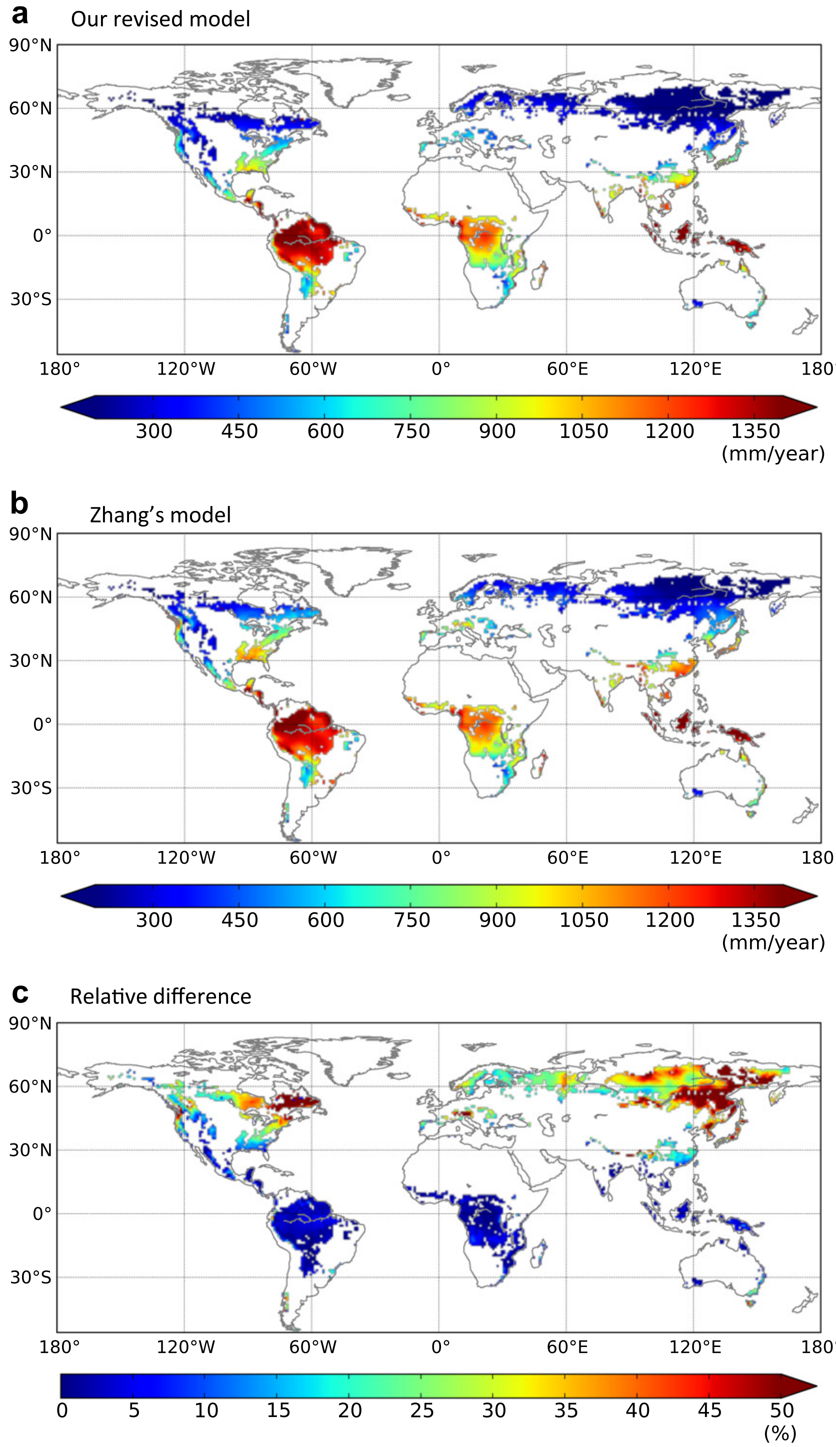

Fig. 8. Global variations in the mean of annual forest evapotranspiration (*ET)* during 1990–1999 calculated using (a) the revised model and (b) Zhang's original model. Blue and red areas indicate regions with high and low *ET*, respectively. For these calculations, we used global data for mean annual precipitation (*P*) and temperature (*T*) at $1^\circ \times 1^\circ$ resolution (Ngo-Duc et al., 2005). (c) Global variation in the relative difference between *ET* predicted using the Zhang's model and *ET* predicted using the revised model; i.e., the difference between *ET* values estimated using the revised model and Zhang's model divided by the *ET* value estimated using the revised model. Blue and red areas indicate regions with high and low relative differences, respectively.

and *w* of the revised model simultaneously according to the 829 observation data we collected.

If we determine E_0 and *w* of the revised model for each *T* class to minimize the RMSE in *ET* estimates, E_0 and *w* are determined as shown in Table 3. Although *w* equals 2.0 for four *T* classes, *w* does not equal 2.0 for the other five classes. When using the parameters in Table 3, the slope of the regression line, R^2, and RMSE for all *ET* data are 1.00, 0.731, and 192 mm, respectively. These values are nearly the same as those for the model assuming *w* as 2.0 (see Section 3.2), indicating the validity of assuming *w* as 2.0.

This similarity in model predictability for different *w* parameterizations is explained by the similarity in the relationships between *P* and forest *ET* predicted using different parameterizations of the model. Fig. 13 shows the relationship between *P* and

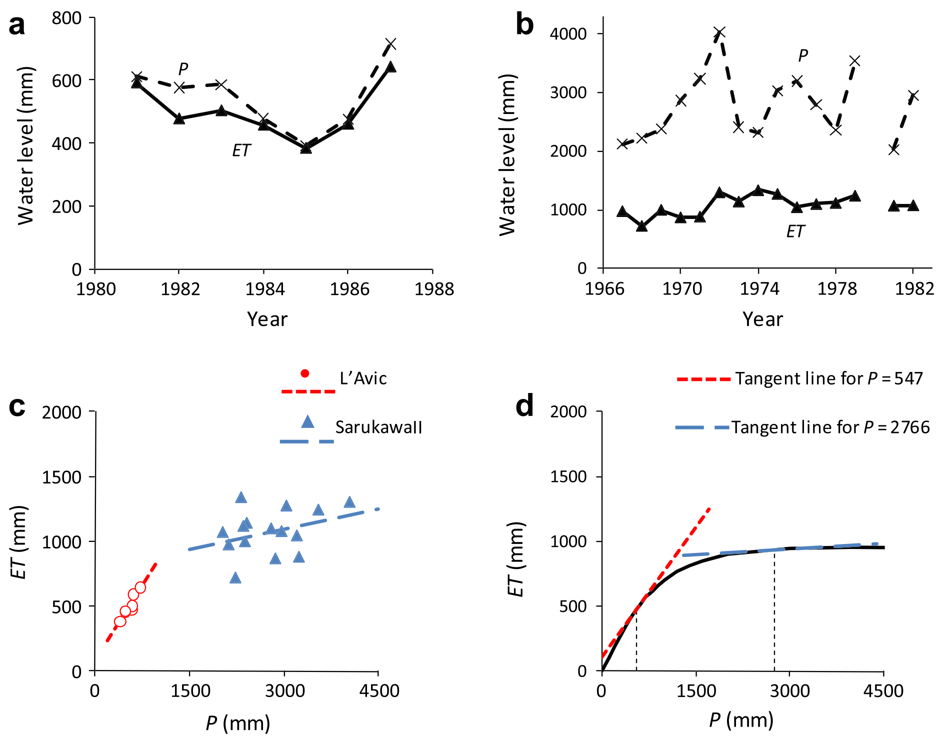

Fig. 9. Sensitivity of annual forest evapotranspiration (*ET*) to annual precipitation (*P*). (a and b) Time-series of *P* and *ET* for two contrasting sites: L'Avic and Sarukawa II, respectively. (c) Relationships between *P* and *ET* for the two sites. The regression line, determined using the least-squares method, was $y = 0.777x - 76.7$ ($R^2 = 0.890$) for the L'Avic site and $y = 0.103x + 792$ ($R^2 = 0.118$) for the Sarukawa II site. (d) Relationship between *P* and *ET* predicted using the revised model (solid line). For model prediction, we assumed annual mean temperature (*T*) as 13.5 °C, which was the mean value for the two sites. Tangent lines for *P* = 548 and 2766 mm are also indicated (dotted and broken lines, respectively).

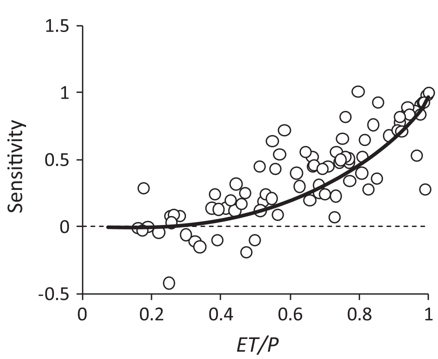

Fig. 10. Relationship of the sensitivity of annual forest evapotranspiration (*ET*) to annual precipitation (*P*) with *ET*/ *P*. The solid line indicates the relationship predicted by the revised model. Circles indicate observed data. *ET*/*P* for the observed data were calculated using the mean *ET* and *P* values for the measurement period.

ET predicted using the model for the class with *T* = 0–5 °C and E_0 and *w* in Table 3. This relationship is nearly identical to that using E_0 in Eq. (2) assuming *T* = 2.5 °C and *w* = 2.0. Although there is some difference between the relationships for *P* greater than 2000 mm, data for which *P* is greater than 2000 mm account for less than 3% of the data for the *T* class. Thus, the difference between the relationships for *P* greater than 2000 mm has little effect on the predictability of the model. Such similarity in the relationship between *P* and *ET* for different *w* parameterizations is observed for the other *T* classes.

4.4. Comparison with previous studies examining the sensitivity of ET to P

There have been many previous studies examining the sensitivity of *ET* to temporal variations in *P* (Koster and Suarez, 1999; Yang et al., 2007; Potter and Zhang, 2009), because such examinations are critical for predicting changes in the terrestrial water cycle corresponding to possible changes in precipitation. The sensitivity of *ET* to *P* relates the sensitivity of annual runoff to temporal variations in *P*, because annual runoff primarily approximates to *P* minus *ET* (Koster and Suarez, 1999; Arora, 2002). When *ET* is sensitive to *P*, the change in *P* is mainly reflected in a change in *ET*, and the annual runoff is therefore insensitive to temporal variations in *P*. When *ET* is insensitive to *P*, the change in *P* is not reflected in a change in *ET*, and the annual runoff is therefore sensitive to temporal variations in *P*.

The relationship of the sensitivity with *ET*/*P* shown in Fig. 10 is expected from the results of several previous studies. Koster and Suarez (1999) and Arora (2002), conducting simulations using climate and/or hydrological models, have already pointed out the relationships of the aridity index (E_0/P) with *ET*/*P* and with the sensitivity of *ET* to temporal variations in *P*, implying a relationship of the sensitivity with *ET*/*P*. These relationships have been validated with field observation data for a specific region (Sankarasubramanian and Vogel, 2003; Potter and Zhang, 2009). Thus, the novelty of the present study is that we used numerous observation data recorded around the world to validate the relationship of the sensitivity with *ET*/*P*. We also showed that the relationship can be derived from the simple model (Eqs. (1) and (2)), suggesting the usefulness of the model in explaining temporal variations in *ET* corresponding to temporal variations in *P*.

4.5. Implications for modeling ET for herbaceous vegetation

Zhang' model includes the forest and herbaceous components. This study showed that considering the dependency of E_0 on *T* is useful for improving predictability of the forest component. This

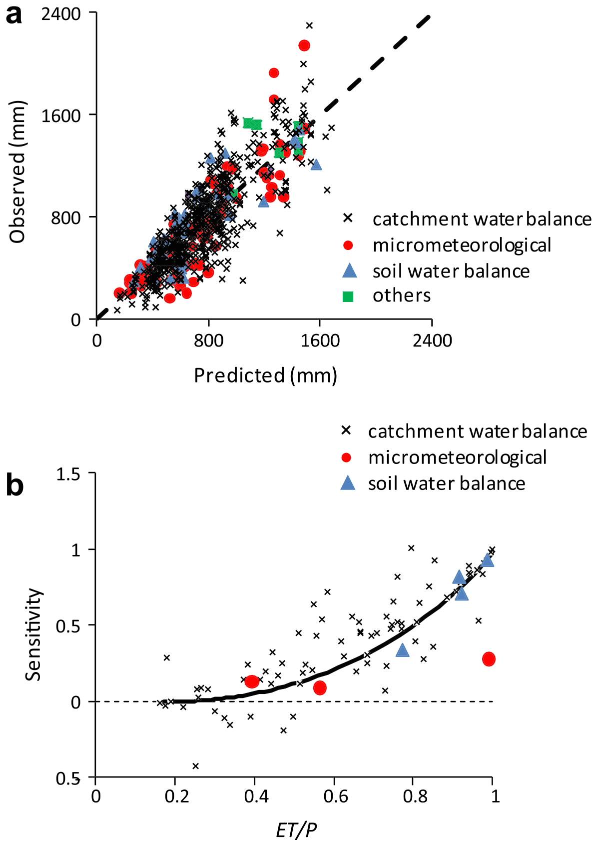

Fig. 11. (a) Comparison between annual forest evapotranspiration (*ET*) predicted using our revised model and observed *ET*. (b) Relationship of the sensitivity of *ET* to annual precipitation (*P*) with *ET*/*P*. The data are classified according to the measurement method.

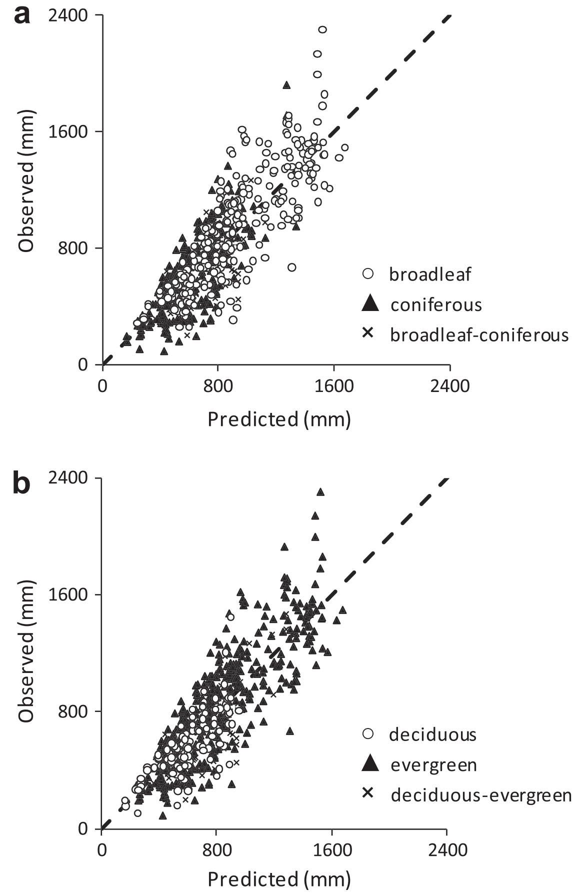

Fig. 12. Comparison between annual forest evapotranspiration (*ET*) predicted using our revised model and observed *ET*. The data are classified according to (a) leaf shape (broadleaf/coniferous) and (b) phenology (deciduous/evergreen).

suggests that similar treatment would be useful for improving predictability of the herbaceous component.

Zhang's model tended to overestimate forest *ET* for mid- and high-latitude forests under low *T* conditions (Fig. 3 and 4). Similar overestimation is observed for mid- and high-latitude herbaceous vegetation (Balonishnikova et al., 2004; Marsh et al., 2004; Seuna and Linjama, 2004; Marc and Robinson, 2007). Marc and Robinson (2007) measured *P* and annual runoff for the Wye catchment in United Kingdom, which was covered with grassland. The mean *P* is 2599 mm and the mean *ET* calculated by *P* minus annual runoff is 488 mm (Marc and Robinson, 2007). *ET* predicted using the herbaceous component of Zhang's model is 881 mm. The overestimation accounts for 81% of the observed *ET*. Similarly, Marsh et al. (2004) measured *P* and annual runoff for the Trail Valley Creek catchment in Canada, which was covered with tundra vegetation. The mean *P* is 231 mm and the mean *ET* calculated by *P* minus annual runoff is 110 mm (Marsh et al., 2004). *ET* predicted using the herbaceous component of Zhang's model is 217 mm. This overestimation accounts for 97% of the observed *ET*. Thus, we recommend studies which extensively collect *ET* data for herbaceous vegetation and formulating E_0 as a function of *T* using the data.

4.6. Other possible application

Our results show that the revised model improves the predictability of the global variation in forest *ET*, because it considers the dependency of E_0 on *T*. Besides this usefulness, the revised model is useful as a simple framework to understand the spatial variations in forest *ET*. Coupling the model with models for other data, such as carbon fixation (Lieth, 1975; Grosso et al., 2008) and species richness (Hawkins et al., 2003; Kreft and Jetz, 2007), will enable more comprehensive understanding of forest ecosystems at a global scale. For example, Grosso et al. (2008) developed a simple model to estimate net primary production (NPP) for forested ecosystems with the input of *P* and *T*. Coupling the revised model and the model of Grosso et al. (2008) clarifies spatial variations in water-use efficiency (NPP divided by *ET*) caused by the spatial variations in *P* and *T*.

Table 3
Annual potential evaporation (E_0) and a coefficient representing plant water availability (*w*) determined for each annual temperature (*T*) class. We assumed that *w* must be between 0.50 and 2.0 in determining E_0 and *w* (Zhang et al., 1999, 2001).

T (°C)	E_0 (mm)	*w*
25–30	1507	2.0
20–25	1301	2.0
15–20	1077	2.0
10–15	974	1.3
5–10	610	2.0
0–5	648	0.62
−5 to 0	473	0.52
−10 to −5	358	0.50
−15 to −10	214	0.50

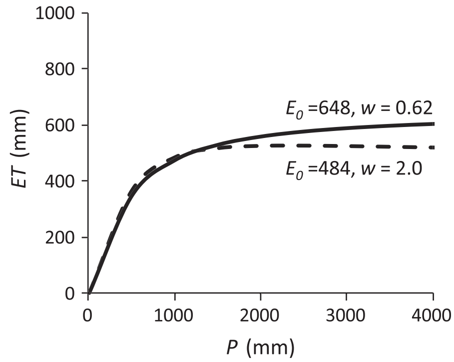

Fig. 13. Relationship between annual precipitation (*P*) and forest evapotranspiration (*ET*) for the class with annual mean temperature (*T*) = 0–5 °C predicted using the model assuming E_0 = 484 mm and *w* = 0.62 (solid line). This figure also shows the relationship between *P* and *ET* predicted using the model assuming E_0 = 648 mm and *w* = 2.0, where this E_0 value is calculated using Eq. (2) assuming *T* = 2.5 °C.

Acknowledgments

Assistance in data collection and compilation provided by Ms. R. Komatsu, Dr. G.-Q. Wang, and Dr. J.-S. Yu are gratefully acknowledged. Thanks are also due to Dr. T. Kume and Dr. W.-L. Liang for their helpful comments. We express sincere thanks to three anonymous reviewers for their constructive comments. This work is funded by a Grant-in-Aid for Scientific Research from the Japanese Ministry of Education, Culture, Sports, Science and Technology and the Research Institute of East Asia Environments, Kyushu University, and by the JSPS Institutional Program for Young Researcher Overseas Visits.

Appendix A. Supplementary material

Supplementary data associated with this article can be found, in the online version, at doi:10.1016/j.jhydrol.2011.12.030.

References

Amthor, J.S., Chen, J.M., Clein, J.S., Frolking, S.E., Goulden, M.L., Grant, R.F., Kimball, J.S., King, A.W., McGuire, A.D., Nikolov, N.T., 2001. Boreal forest CO_2 exchange and evapotranspiration predicted by nine ecosystem process models: intermodel comparisons and relationships to field measurements. J. Geophys. Res. 106, 33623–33648.

Arain, M.A., Black, T.A., Barr, A.G., Griffis, T.J., Morgenstern, K., Nesic, Z., 2003. Year-round observations of the energy and water vapour fluxes above a boreal black spruce forest. Hydrol. Process. 17, 3581–3600.

Arora, V.K., 2002. The use of the aridity index to assess climate change effect on annual runoff. J. Hydrol. 265, 164–177.

Bala, G., Caldeira, K., Wickett, M., Phillips, T.J., Lobell, D.B., Delire, C., Mirin, A., 2007. Combined climate and carbon-cycle effects of large-scale deforestation. Proc. Natl. Acad. Sci. USA 104, 6550–6555.

Balonishnikova, J.A., Krestovsky, O.I., Shutov, V.A., 2004. Water balance of experimental watersheds in the Valdai Branch of the State Hydrological Institute (SHI), Russia. IAHS Publ. 290, 91–102.

Bartholomé, E., Belward, A.S., 2005. GLC2000: a new approach to global land cover mapping from Earth observation data. Int. J. Remote Sens. 26, 1959–1977.

Bigelow, S., 2001. Evapotranspiration modelled from stands of three broad-leaved tropical trees in Costa Rica. Hydrol. Process. 15, 2779–2796.

Blanken, P.D., Black, T.A., Yang, P.C., Neumann, H.H., Nesic, Z., Staebler, R., den Hartog, G., Novak, M.D., Lee, X., 1997. Energy balance and canopy conductance of a boreal aspen forest: partitioning overstory and understory components. J. Geophys. Res. 102, 28915–28927.

Bonan, G.B., 2008. Forests and climate change: forcings, feedbacks, and climate benefits of forests. Science 320, 1444–1449.

Bosch, J.M., Hewlett, J.D., 1982. A review of catchment experiments to determine the effect of vegetation changes on water yield and evapotranspiration. J. Hydrol. 55, 3–23.

Bradshaw, C.J.A., Sodhi, N.S., Peh, K.S.H., Brooks, B.W., 2007. Global evidence that deforestation amplifies flood risk and severity in the developing world. Global Change Biol. 13, 2379–2395.

Brown, A., Zhang, L., McMahon, T.A., Western, A.W., Vertessy, R.A., 2005. A review of paired catchment studies for determining changes in water yield resulting from alterations in vegetation. J. Hydrol. 310, 28–61.

Brown, A.E., Podger, G.M., Davidson, A.J., Dowling, T.I., Zhang, L., 2007. Predicting the impact of plantation forestry on water users at local and regional scales. Forest Ecol. Manage. 251, 82–93.

Budyko, M.I., 1974. Climate and Life. Academic Press, Orlando.

Calder, I.R., Reid, I., Nisbet, T.R., Green, J.C., 2003. Impact of lowland forests in England on water resources: application of the Hydrological Land Use Change (HYLUC) model. Water Resour. Res. 39, 1319.

Choudhury, B.J., 1997. Global pattern of potential evaporation calculated from the Penman–Monteith equation using satellite and assimilated data. Remote Sens. Environ., 61–64.

Cornish, P.M., Vertessy, R.A., 2001. Forest age-induced changes in evapotranspiration and water yield in a eucalypt forest. J. Hydrol. 242, 43–63.

Dooge, J.C.I., Bruen, M., Parmentier, B., 1999. A simple model for estimating the sensitivity of runoff to long-term changes in precipitation without a change in vegetation. Adv. Water Resour. 23, 153–163.

Gerten, D., Schaphoff, S., Haberlandt, U., Lucht, W., Sitch, S., 2004. Terrestrial vegetation and water balance-hydrological evaluation of a dynamic global vegetation model. J. Hydrol. 286, 249–270.

Gielen, B., Verbeeck, H., Neirynck, J., Sampson, D.A., Vermeiren, F., Janssens, I.A., 2010. Decadal water balance of a temperate Scots pine forest (*Pinus sylvestris* L.) based on measurements and modelling. Biogeosciences 7, 1247–1261.

Grosso, S.D., Parton, W., Gren, T.S., Zheng, D., Bachelet, D., Prince, S., Hibbard, K., Olson, R., 2008. Global potential net primary production predicted from vegetation class, precipitation, and temperature. Ecology 89, 2117–2126.

Hamon, W.R., 1961. Estimating potential evapotranspiration. Proc. Am. Soc. Civil Eng. 87, 197–120.

Hansen, M.C., DeFries, R.S., Townshend, J.R.G., Carroll, M., Dimiceli, C., Sohlberg, R.A., 2003. Global percent tree cover at a spatial resolution of 500 meters: first results of the MODIS vegetation continuous fields algorithm. Earth Interact. 7, 1–15.

Hawkins, B.A., Field, R., Cornell, H.V., Currie, D.J., Guegan, J., Kaufman, D.M., Kerr, J.T., Mittelbach, G.G., Oberdorff, T., O'Brien, F., Porter, E.E., Turner, J.R.G., 2003. Energy, water, and broad-scale geographic patterns of species richness. Ecology 84, 3105–3117.

Herron, N., Davis, R., Jones, R., 2002. The effects of large-scale afforestation and climate change on water allocation in the Macquarie River catchment, NSW, Australia. J. Environ. Manage. 65, 369–381.

Huber, A., Iroumé, A., Bathurst, J., 2008. Effect of Pinus radiata plantations on water balance in Chile. Hydrol. Process. 22, 142–148.

Hunt, L.A., Kuchar, L., Swanton, C.J., 1998. Estimation of solar radiation for use in crop modelling. Agric. Forest Meteorol. 91, 293–300.

Iroumé, A., Mayen, O., Huber, A., 2006. Runoff and peak flow responses to timber harvest and forest age in southern Chile. Hydrol. Process. 20, 37–50.

Jung, M., Reichstein, M., Ciais, P., Seneviratne, S.I., Sheffield, J., Goulden, M.L., Bonan, B., Cescatti, A., Chen, J., de Jeu, R., Dolman, A.J., Eugster, W., Gerten, D., Gianelle, D., Gobron, N., Heinke, J., Kimball, J., Law, B.E., Montagnani, L., Mu, Q., Mueller, B., Oleson, K., Papale, D., Richardson, A.D., Roupsard, O., Running, S., Tomelleri, E., Viovy, N., Weber, U., Williams, C., Wood, E., Zaehle, S., Zhang, K., 2010. Recent decline in the global land evapotranspiration trend due to limited moisture supply. Nature 467, 951–954.

Komatsu, H., Tanaka, N., Kume, T., 2007. Do coniferous forests evaporate more water than broad-leaved forests in Japan? J. Hydrol. 336, 361–375.

Komatsu, H., Kume, T., Otsuki, K., 2008a. The effect of converting a native broad-leaved forest to a coniferous plantation forest on annual water yield: a paired-catchment study in northern Japan. Forest Ecol. Manage. 255, 880–886.

Komatsu, H., Maita, E., Otsuki, K., 2008b. A model to estimate annual forest evapotranspiration in Japan from mean annual temperature. J. Hydrol. 348, 330–340.

Komatsu, H., Kume, T., Otsuki, K., 2010a. A simple model to estimate monthly forest evapotranspiration in Japan from monthly temperature. Hydrol. Process. 24, 1896–1911.

Komatsu, H., Kume, T., Shinohara, Y., Miyazawa, Y., Otsuki, K., 2010b. Did annual run-off and low flow decrease with reduced forestry practices in Japan? Hydrol. Process. 24, 2440–2451.

Komatsu, H., Kume, T., Otsuki, K., 2011. Increasing annual runoff–broadleaf or coniferous forests? Hydrol. Process. 25, 302–318.

Koster, R.D., Suarez, M.J., 1999. A simple framework for examining the interannual variability of land surface moisture fluxes. J. Clim. 12, 1911–1917.

Kosugi, Y., Katsuyama, M., 2007. Evapotranspiration over a Japanese cypress forest. II. Comparison of the eddy covariance and water budget methods. J. Hydrol. 334, 305–311.

Kreft, H., Jetz, W., 2007. Global patterns and determinants of vascular plant diversity. Proc. Natl. Acad. Sci. USA 104, 5925–5930.

Kumagai, T., Katul, G., Saitoh, T.M., Sato, Y., Manfroi, O.J., Morooka, T., Ichie, T., Kuraji, K., Suzuki, M., Porporato, A., 2004. Water cycling in a Bornean tropical rain forest under current and projected precipitation scenarios. Water Resour. Res. 40, W01104.

Landsberg, J.J., Gower, S.T., 1997. Applications of Physiological Ecology to Forest Management. Academic Press, San Diego.

Law, B.E., Falge, E., Gu, L., Baldocchi, D.D., Bakwin, P., Berbigier, P., Davis, K., Dolman, A.J., Falk, M., Fuentes, J.D., Goldstein, A., Granier, A., Grelle, A., Hollinger, D., Janssens, I.A., Jarvis, P., Jensen, N.O., Katul, G., Mahli, Y., Matteucci, G., Meyers, T., Monson, R., Munger, W., Oechel, W., Olson, R., Pilegaard, K., Paw, U., K.T., Thorgeirsson, H., Valentini, R., Verma, S., Vesala, T., Wilson, K., Wofsy, S., 2002. Environmental controls over carbon dioxide and water vapour exchange of terrestrial vegetation. Agric. Forest Meteorol., 113, 97–120.

Leuning, R., 1990. Modelling stomatal behaviour and photosynthesis of *Eucalyptus grandis*. Aust. J. Plant Physiol. 17, 159–175.

Leuning, R., 1995. A critical appraisal of a combined stomatal-photosynthesis model for C3 plants. Plant, Cell Environ. 18, 339–355.

Lieth, H., 1975. Modeling the primary productivity of the world. In: Lieth, H., Whittaker, R.H. (Eds.), Primary Productivity of the Biosphere. Springer-Verlag, New York, pp. 237–264.

Loescher, H.W., Gholz, H.L., Jacobs, J.M., Oberbauer, S.F., 2005. Energy dynamics and modeled evapotranspiration from a wet tropical forest in Costa Rica. J. Hydrol. 315, 274–294.

Lu, J., Sun, G., McNulty, S.G., Amatya, D.M., 2003. Modeling actual evapotranspiration from forested watersheds across the Southeastern United States. J. Am. Water Resour. Assoc. 39, 887–896.

Maita, E., Suzuki, M., Ohta, T., 2005. Change in the annual discharge after clear-cutting a 70-year-old mixed plantation of Sugi and Hinoki in a Tertiary formation area. J. Jpn. Forest Soc. 87, 124–132 (in Japanese with English summary).

Malmer, A., 1992. Water-yield changes after clear-felling tropical rainforest and establishment of forest plantation in Sabah, Malaysia. J. Hydrol. 134, 77–94.

Marc, V., Robinson, M., 2007. The long-term water balance (1972–2004) of upland forestry and grassland at Plynlimon, mid-Wales. Hydrol. Earth Syst. Sci. 11, 44–60.

Marsh, P., Onclin, C., Russell, M., 2004. A multi-year hydrological data set for two research basins in the Mackenzie Delta region, NW Canada. IAHS Publ. 290, 205–212.

Matsumoto, K., Ohta, T., Nakai, T., Kuwada, T., Daikoku, K., Iida, S., Yabuki, H., Kononov, A.V., van der Molen, M.K., Kodama, Y., Maximov, T.C., Dolman, J.A., Hattori, S., 2008. Energy consumption and evapotranspiration at several boreal and temperate forests in the Far East. Agric. Forest Meteorol. 148, 1978–1989.

McJannet, D., Wallece, J., Fitch, P., Disher, M., Reddell, P., 2007. Water balance of tropical rainforest canopies in north Queensland, Australia. Hydrol. Process. 21, 3473–3483.

Melillo, J.M., McGuire, A.D., Kicklighter, D.W., Moore III, B., Vorosmarty, C.J., Schloss, A.L., 1993. Global climate change and terrestrial net primary production. Nature 363, 234–240.

Meza, F., Varas, E., 2000. Estimation of mean monthly solar global radiation as a function of temperature. Agric. Forest Meteorol. 100, 231–241.

Milly, P.C.D., 1994. Climate, soil water storage, and the average annual water balance. Water Resour. Res. 30, 2143–2156.

Mu, Q., Heinsch, F.A., Zhao, M., Running, S.W., 2007. Development of a global evapotranspiration algorithm based on MODIS and global meteorology data. Remote Sens. Environ. 111, 519–536.

Muller, J., 2009. Forestry and water budget of the lowlands in northeast Germany – consequences for the choice of tree species and for forest management. J. Water Land Dev. 13, 133–148.

Ngo-Duc, T., Polcher, J., Laval, K., 2005. A 53-year forcing data set for land surface models. J. Geophys. Res. 110, D06116.

Nordblom, T., Hume, I., Bathgate, A., Reynolds, M., 2006. Mathematical optimisation of drainage and economic land use for target water and salt yields. Aust. J. Agric. Resour. Econom. 50, 381–402.

Oishi, A.C., Oren, R., Novick, K.A., Palmroth, S., Katul, G.G., 2010. Interannual invariability of forest evapotranspiration and its consequence to water flow downstream. Ecosystems 13, 421–436.

Oki, T., Kanae, S., 2006. Global hydrological cycles and world water resources. Science 313, 1068–1072.

Pearce, A.J., Rowe, L.K., O'Loughlin, C.L., 1982. Hydrologic regime of undisturbed mixed evergreen forest, South Nelson, New Zealand. J. Hydrol. (NZ) 21, 98–116.

Piñol, J., Lledó, M.J., Escarré, A., 1991. Hydrological balance of two Mediterranean forested catchments (Prades, northeast Spain). Hydrol. Sci. J. 36, 95–107.

Potter, N.J., Zhang, L., 2009. Interannual variability of catchment water balance in Australia. J. Hydrol. 369, 120–129.

Rowe, L.K., Pearce, A.J., 1994. Hydrology and related changes after harvesting native forest catchments and establishing pinus radiata plantations. Part 2. The native forest water balance and changes in streamflow after harvesting. Hydrol. Process. 8, 281–297.

Ruprecht, J.K., Schofiel, N.J., Crombie, D.S., Vertessy, R.A., Stoneman, G.L., 1991. Early hydrological response to intense forest thinning in southwestern Australia. J. Hydrol. 127, 261–277.

Sankarasubramanian, A., Vogel, R.M., 2003. Hydroclimatology of the continental United States. Gephys. Res. Lett. 30, 1363.

Schellekens, J., 2000. Hydrological Processes in A Humid Tropical Rain Forest: A Combined Experimental and Modelling Approach. PhD Thesis, Vrije Universiteit, Amsterdam.

Schellekens, J., Bruijnzeel, L.A., Scatena, F.N., Bink, N.J., Howerda, F., 2000. Evaporation from a tropical rain forest, Luquillo Experimental Forest, eastern Puerto Rico. Water Resour. Res. 36, 2183–2196.

Schreiber, P., 1904. Uber die Beziehungen zwischen dem Niederschalag und der Wasserfuhrung der Flusse in Mitteleuropa. Z. Meteorol. 21, 441–452.

Seuna, P., Linjama, J., 2004. Water balances of the northern catchments of Finland. IAHS Publ. 290, 111–119.

Sharda, V.N., Samraj, P., Samra, J.S., Lakshmanan, V., 1998. Hydrological behaviour of first generation coppiced bluegum plantations in the Nilgiri sub-watersheds. J. Hydrol. 211, 50–60.

Shimizu, A., Shimizu, T., Miyabuchi, Y., Ogawa, Y., 2003. Evapotranspiration and runoff in a forest watershed, western Japan. Hydrol. Process. 17, 3125–3149.

Shinohara, Y., Komatsu, H., Otsuki, K., 2007. A method for estimating global solar radiation from daily maximum and minimum temperatures: its applicability to Japan. J. Jpn. Soc. Hydrol. Water Resour. 20, 462–469 (in Japanese with English summary).

Sitch, S., Smith, B., Prentice, I.C., Arneth, A., Bondeau, A., Cramer, W., Kaplan, J.O., Levis, S., Lucht, W., Sykes, M.T., Thonicke, K., Venevsky, S., 2003. Evaluation of ecosystem dynamics, plant geography and terrestrial carbon cycling in the LPJ dynamic global vegetation model. Global Change Biol. 9, 161–185.

Sun, G., McNulty, S.G., Lu, J., Amatya, D.M., Liang, Y., Kolka, R.K., 2005. Regional annual water yield from forest lands and its response to potential deforestation across the southeastern United States. J. Hydrol. 308, 258–268.

Sun, G., Zhou, G., Zhang, Z., Wei, X., McNulty, S.G., Vose, J.M., 2006. Potential water yield reduction due to forestation across China. J. Hydrol. 328, 548–558.

Sun, G., Alstad, K., Chen, J., Chen, S., Ford, C.R., Lin, G., Liu, C., Lu, N., McNulty, S.G., Miao, H., Noormets, A., Vose, J.M., Wilske, B., Zeppel, M., Zhang, Y., Zhang, Z., 2011. A general predictive model for estimating monthly ecosystem evapotranspiration. Ecohydrology 4, 245–255.

Syvitski, J.P.M., Vörösmarty, J., Kettner, A.J., Green, P., 2005. Impact of humans on the flux of terrestrial sediment to the global coastal ocean. Science 308, 376–380.

Takeshita, K., Shimizu, A., Miyabuchi, Y., 1996. Statistical report of hydrological observation at Sarukawa experimental watershed. Bull. FFPRI 370, 31–75 (in Japanese).

Thornthwaite, C.W., 1948. An approach toward a rational classification of climate. Geogr. Rev. 38, 55–94.

Thornton, P.E., Running, S.W., 1999. An improved algorithm for estimating incident daily solar radiation from measurements of temperature, humidity, and precipitation. Agric. Forest Meteorol. 93, 211–228.

Turner, K.M., 1991. Annual evapotranspiration of native vegetation in a Mediterranean-type climate. Water Resour. Bull. 27, 1–6.

Van der Salm, C., van der Gon, H.D., Wieggers, R., Bleeker, A., van den Toorn, A., 2006. The effect of afforestation on water recharge and nitrogen leaching in The Netherlands. Forest Ecol. Manage. 221, 170–182.

van Wijk, T.M., Dekker, J.C., Bouten, W., Kohsiek, W., Mohren, G.M.J., 2001. Simulation of carbon and water budgets of a Douglas-fir forest. Forest Ecol. Manage. 145, 229–241.

Wang, E., Yu, Q., Wu, D., Xia, J., 2008. Climate, agricultural production and hydrological balance in the North China Plain. Int. J. Clim. 28, 1959–1970.

Ward, R.C., Robinson, M., 2000. Principles of Hydrology. McGraw-Hill, London.

Wilson, K.B., Baldocchi, D.D., 2000. Seasonal and interannual variability of energy fluxes over a broadleaved temperate deciduous forest in North America. Agric. Forest Meteorol. 100, 1–18.

Wilson, K.B., Hason, P.J., Mulholland, P.J., Baldocchi, D.D., Wullschleger, S.D., 2001. A comparison of methods for determining forest evapotranspiration and its components: sap-flow, soil water budget, eddy covariance and catchment water balance. Agric. Forest Meteorol. 106, 153–168.

Yang, D., Sun, F., Liu, Z., Cong, Z., Ni, G., Lei, Z., 2007. Analyzing spatial and temporal variability of annual water-energy balance in nonhumid regions of China using the Budyko hypothesis. Water Resour. Res. 43, W04426.

Zhang, L., Dawes, W.R., Walker, G.R., 1999. Predicting the Effect of Vegetation Changes on Catchment Average Water Balance. Cooperative Research Centre for Catchment Hydrology Technical Report 99/12.

Zhang, L., Dawes, W.R., Walker, G.R., 2001. Response of mean annual evapotranspiration to vegetation changes at catchment scale. Water Resour. Res. 37, 701–708.

Zhang, K., Kimball, J.S., Nemani, R.R., Running, S.W., 2010. A continuous satellite – derived global record of land surface evapotranspiration from 1983 to 2006. Water Resour. Res. 46, W09522.